LCLUC Meeting, Maryland, April 2014

Mega Urban Changes and Impacts in the Decade of the 2000s

Interdisciplinary Research in Earth Science (IDS)
Authors and Contributors from IDS Science Team

Presentation by Son V. Nghiem (PI)

Jet Propulsion Laboratory
California Institute of Technology
Pasadena, California, USA

Interdisciplinary Science Team

PI: Son V. Nghiem, Jet Propulsion Laboratory, California Institute of Technology, CA, USA.

Co-Is: Mark Jacobson, Stanford University, CA, USA; Chris Small, LDEO, Columbia University, NY, USA; Deborah Balk, City University of New York, USA.

Collaborators: Marco Masetti, University of Milan, Italy; Alessandro Sorichetta and Andy Tatem, University of Southampton, UK; Catherine Linard, University of Brussels, Belgium; Dorothy Hall, NASA GSFC, USA; Andreas Richter, University of Bremen, Germany; Uwe Deichmann, The World Bank; Kevin Gurney, Arizona State University, USA, Paul Shepson, Purdue University, USA; Chris Field, Carnegie Institution, USA; Paolo Fabbri and Marco Pola, University of Padova, Italy; Alessandro Gargini, University of Bologna, Italy; Fulvio Celico, University of Parma, Italy; Marco Deserti, ARPA Emilia Romagna, Italy; Paolo Pampaloni and Simonetta Paloscia, IFAC-CNR, Italy; Robert Brakenridge, University of Colorado, USA; Paul Morin, University of Minnesota, USA.

Objective and Approach

- **Objective:** Investigate impacts of global urban changes on the environment during the rapid growth of large cities (mega-urbanization) in the decade of the 2000s, including:
  Physical factors: urban heat island, urban dome, emission, pollutions in the atmosphere and water systems.
  Demographic factors: population distribution, population dynamics and changes in livelihoods such as housing, living arrangements, and socioeconomic status.
- **Approach:** Four components
  1. Satellite observations: >15 satellites
  2. Surface networks: meteorological, hydrological, chemical
  3. Socioeconomics and demography data
  4. Modeling: Gas, Aerosol, Transport, Radiation, General Circulation, Mesoscale, and Ocean Model (GATOR-GCMOM).
- **Field Campaign:** POPLEX Field Campaign, Italy, May 2014.

Dense Sampling Method
(Patent US 8,401,793 B2, 3/19/2013)

Enable global urban observations without gaps

$$P_{Ri} = \frac{P_{Ti}\lambda^2}{(4\pi)^3 R^4} \iint_A dx\, dy\, G(\phi_i, x, y)\, \sigma_0(\phi_i, t_i, x, y)$$

$$P_{Ri} = \frac{P_{Ti}\lambda^2}{(4\pi)^3 R^4}\, \overline{\sigma}_0(\phi_i, t_i) \iint_A dx\, dy\, G(\phi_i, x, y)$$

$$\overline{\sigma}_0(\phi_i, t_i) = \frac{1}{\Gamma_A} \iint_A dx\, dy\, G(\phi_i, x, y)\, \sigma_0(\phi_i, t_i, x, y)$$

Dense Sampling Method
(Patent US 8,401,793 B2, 3/19/2013)

Enable global urban observations without gaps

$$\overline{\sigma}_0 = \frac{1}{N}\sum_{i=1}^{N}\overline{\sigma}_0(\phi_i, t_i) = \frac{1}{N\Gamma_A}\sum_{i=1}^{N}\iint_A dx\,dy\,G(\phi_i, x, y)\,\sigma_0(\phi_i, t_i, x, y)$$

$$\sigma_0(\phi_i, t_i, x, y) = \overline{\sigma}_0(x, y) + \varepsilon(\phi_i, t_i, x, y)$$

$$\overline{\sigma}_{0M} = \frac{1}{\Gamma_A}\iint_A dx\,dy\left[\sum_{i=1}^{N}\frac{G(\phi_i, x, y)}{N}\right]\overline{\sigma}_0(x, y)$$

$$\mathcal{R} = \frac{1}{\Gamma_A}\iint_A dx\,dy\sum_{i=1}^{N}\left[\frac{G(\phi_i, x, y)}{N}\,\varepsilon(\phi_i, t_i, x, y)\right]$$

Verification - Príncipe Island

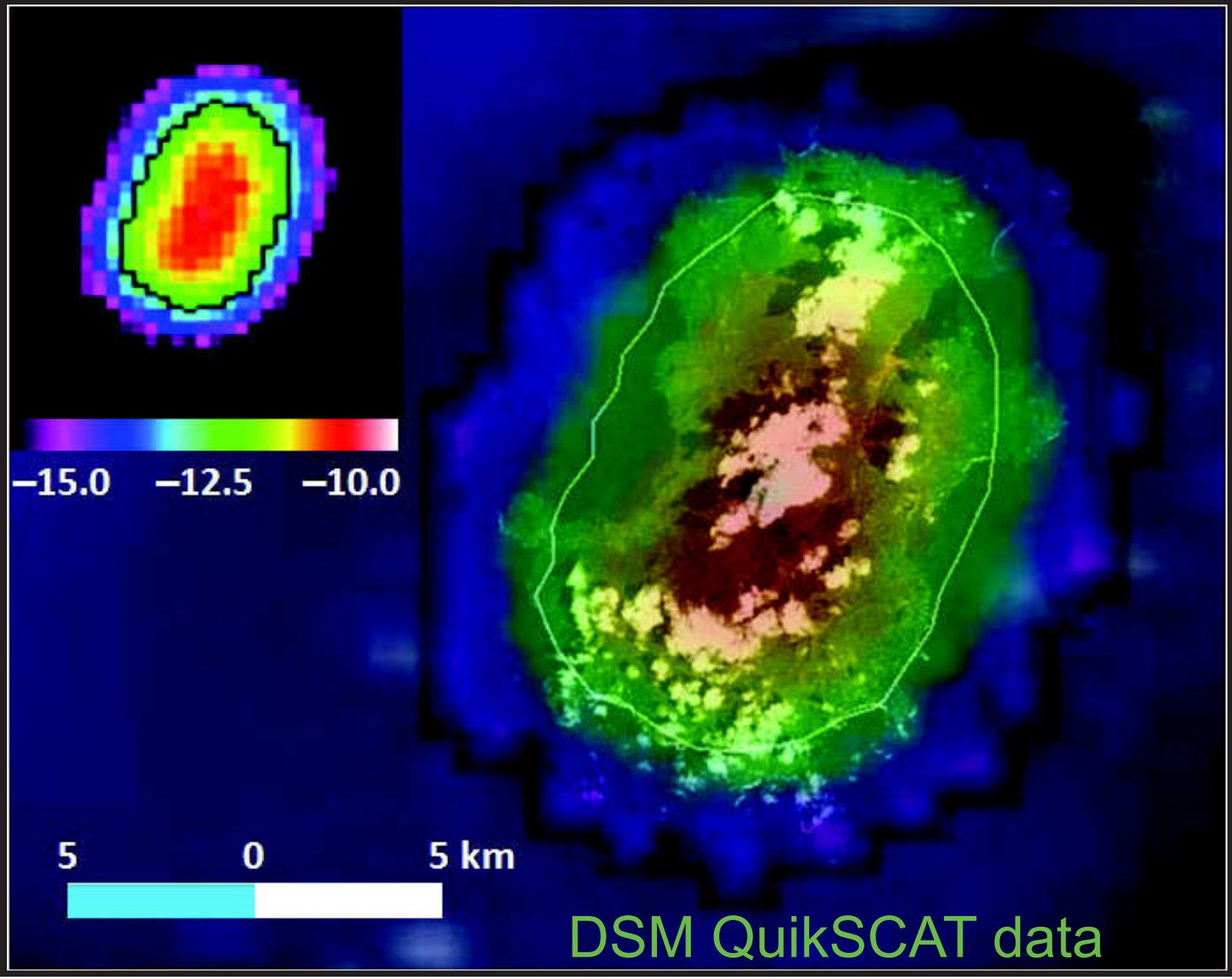

Procedure to Obtain Global Urban Extent, Type, Change

- Use the DECADE of NASA QuikSCAT satellite scatterometer collected GLOBALLY
- Apply the Dense Sampling Method for high-resolution data processing over land regions
- Classification using training urban data from multiple sources, using both mean and variation
- Verification in regions where census/demo-graphic data are available (e.g. Dallas-Ft Worth)
- Obtain urban extent, and typology (commercial/ industrial core, residential, rural), and change

Enable Development of ATLAS of Global Urban Change

DSM: All Mega Cities Worldwide

Rank	Megacity	Country	Continent	Population	DSM Latitude (°)		DSM Longitude (°)	
1	Tokyo	Japan	Asia	34,800,000	33.8	37.9	137.5	142.3
2	Guangzhou	China	Asia	31,700,000	21.0	25.0	111.2	115.5
3	Shanghai	China	Asia	28,900,000	30.4	31.9	120.4	122.6
4	Jakarta	Indonesia	Asia	26,400,000	-6.8	-5.6	106.1	107.5
5	Seoul	South Korea	Asia	25,800,000	37.0	38.0	126.3	127.8
6	Delhi	India	Asia	24,000,000	28.2	29.1	76.6	77.7
7	Mexico City	Mexico	North America	23,800,000	18.4	20.5	-99.9	-98.1
8	Karachi	Pakistan	Asia	22,700,000	24.4	25.2	66.5	67.6
9	Manila	Philippines	Asia	22,200,000	14.0	15.2	120.6	121.5
10	New York City	United States	North America	21,600,000	39.9	41.5	-76.1	-71.6
11	São Paulo	Brazil	South America	21,500,000	-24.2	-22.9	-47.6	-45.5
12	Mumbai	India	Asia	21,400,000	18.5	19.7	72.6	73.4
13	Beijing	China	Asia	19,300,000	39.2	40.7	115.5	117.3
14	Los Angeles	United States	North America	17,200,000	32.8	34.9	-120.0	-116.2
15	Osaka	Japan	Asia	16,800,000	33.8	35.4	134.2	136.4
16	Moscow	Russia	Europe	16,500,000	55.3	56.2	36.9	38.4
17	Dhaka	Bangladesh	Asia	16,300,000	23.4	24.1	90.1	90.7
18	Cairo	Egypt	Africa	16,100,000	29.7	30.4	30.8	31.7
19	Kolkata	India	Asia	16,000,000	21.9	23.3	87.7	88.8
20	London	United Kingdom	Europe	15,500,000	51.0	52.0	-1.1	1.0
21	Buenos Aires	Argentina	South America	14,500,000	-35.4	-33.9	-59.5	-57.2
21	Bangkok	Thailand	Asia	14,500,000	13.0	14.8	99.7	101.3
23	Istanbul	Turkey	Europe/Asia	13,800,000	40.4	41.6	27.9	30.2
24	Lagos	Nigeria	Africa	13,200,000	6.0	7.3	2.7	4.2
25	Tehran	Iran	Asia	13,200,000	35.3	36.1	50.8	51.9
26	Rio de Janeiro	Brazil	South America	12,900,000	-23.4	-22.3	-44.2	-42.4
27	Shenzhen	China	Asia	11,700,000	21.5	24.0	112.4	115.0
28	Paris	France	Europe	10,700,000	48.5	49.2	1.7	2.9
29	Tianjin	China	Asia	10,600,000	38.6	39.6	116.6	118.0

Beijing DSM Backscatter

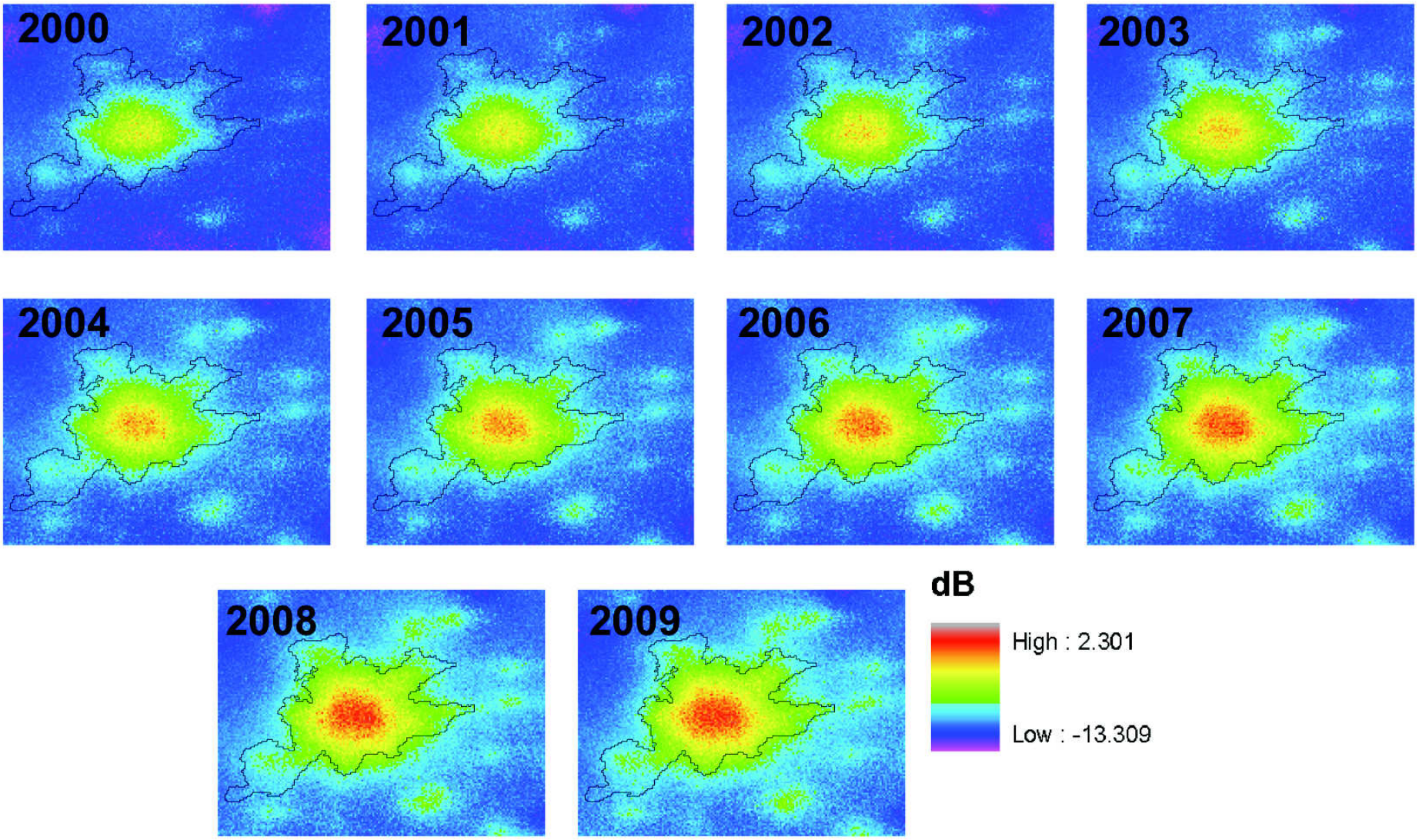

Paper in preparation

Beijing DSM Index of Variability

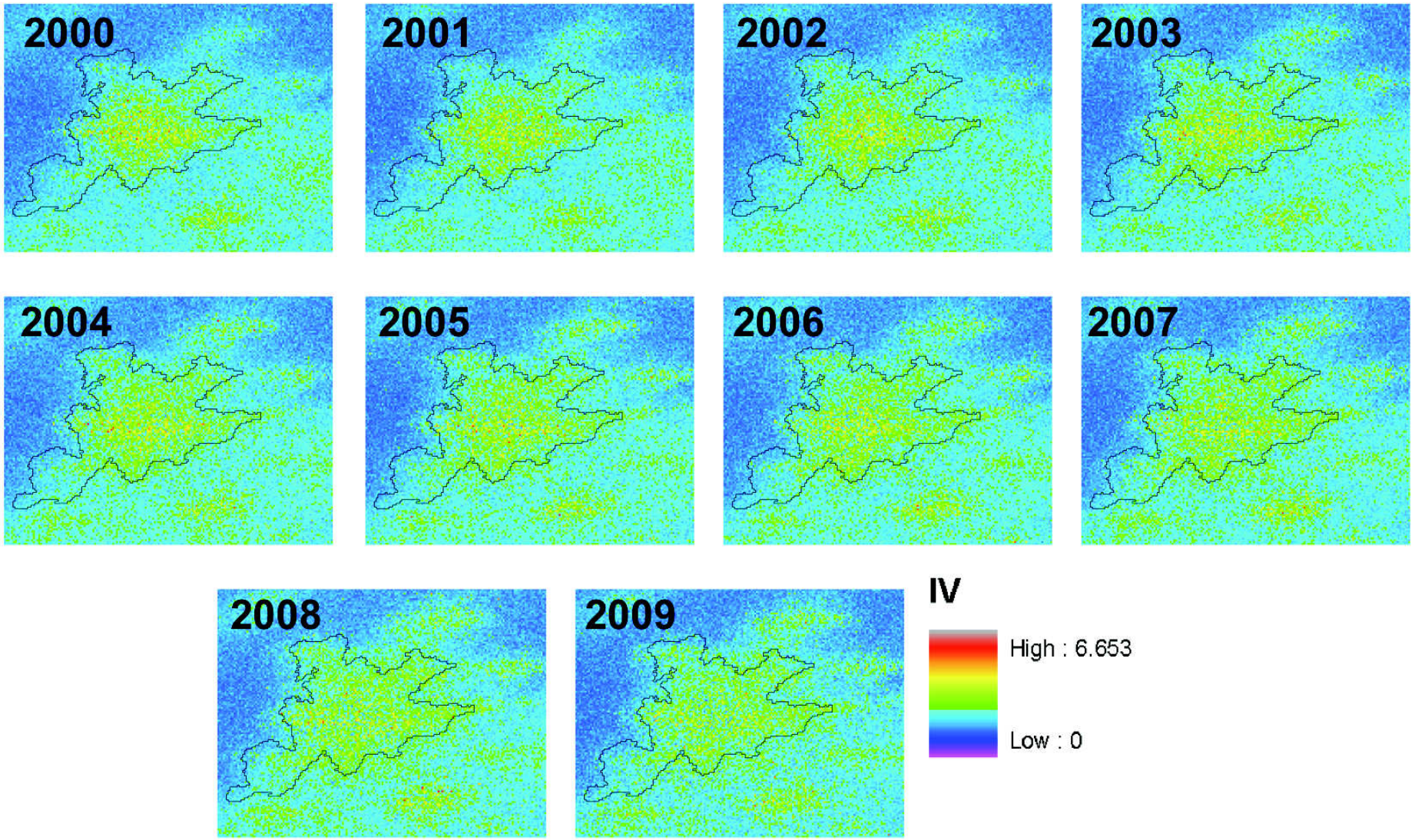

Paper in preparation

Rate of Change – DSM 2000-09

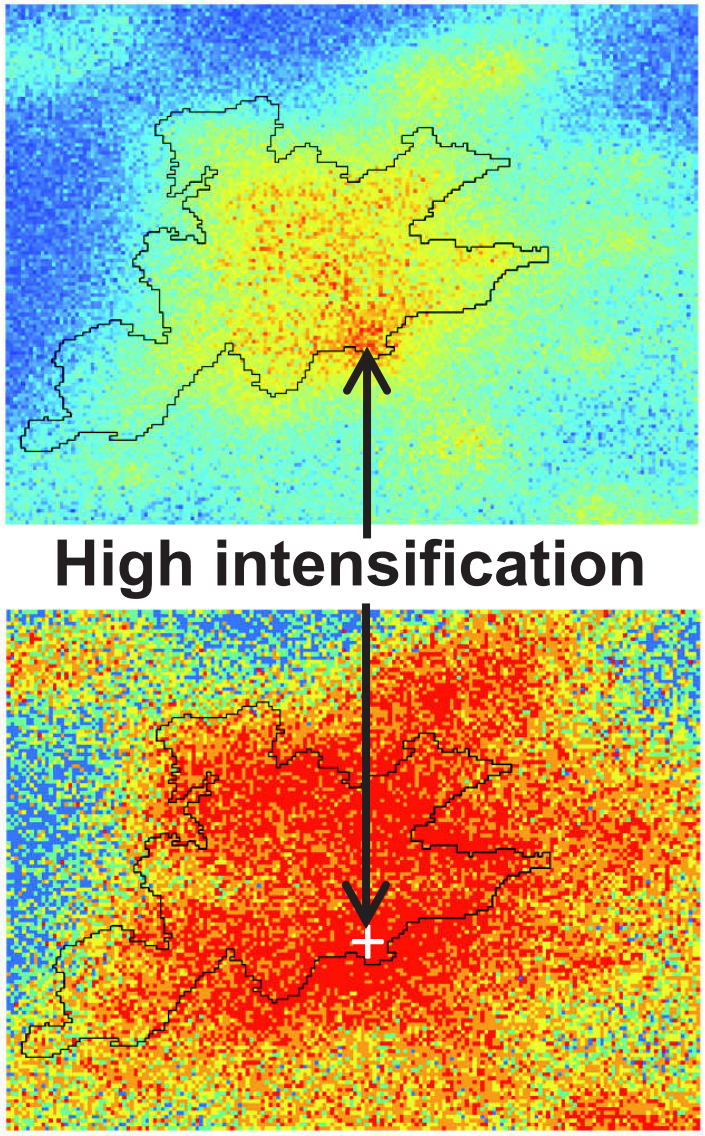

SLOPE (Trend)

R^2

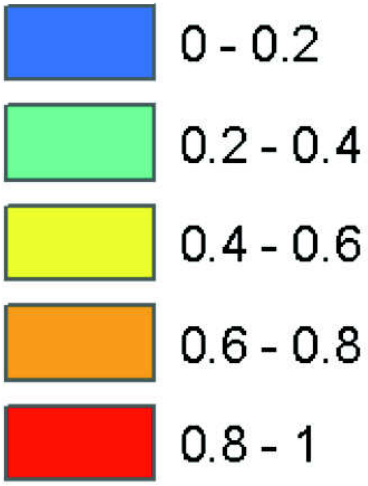

Paper in preparation

Very Significant Build-up in an Area in Southeast Beijing

Center of image is located around 39°46′40″ N and 116°31′29″ E (marked by the white plus in the 2000-2009 DSM R^2 images)

Images from Google Earth Pro 5.1

Paper in preparation

Beijing Urban Extent from DSM

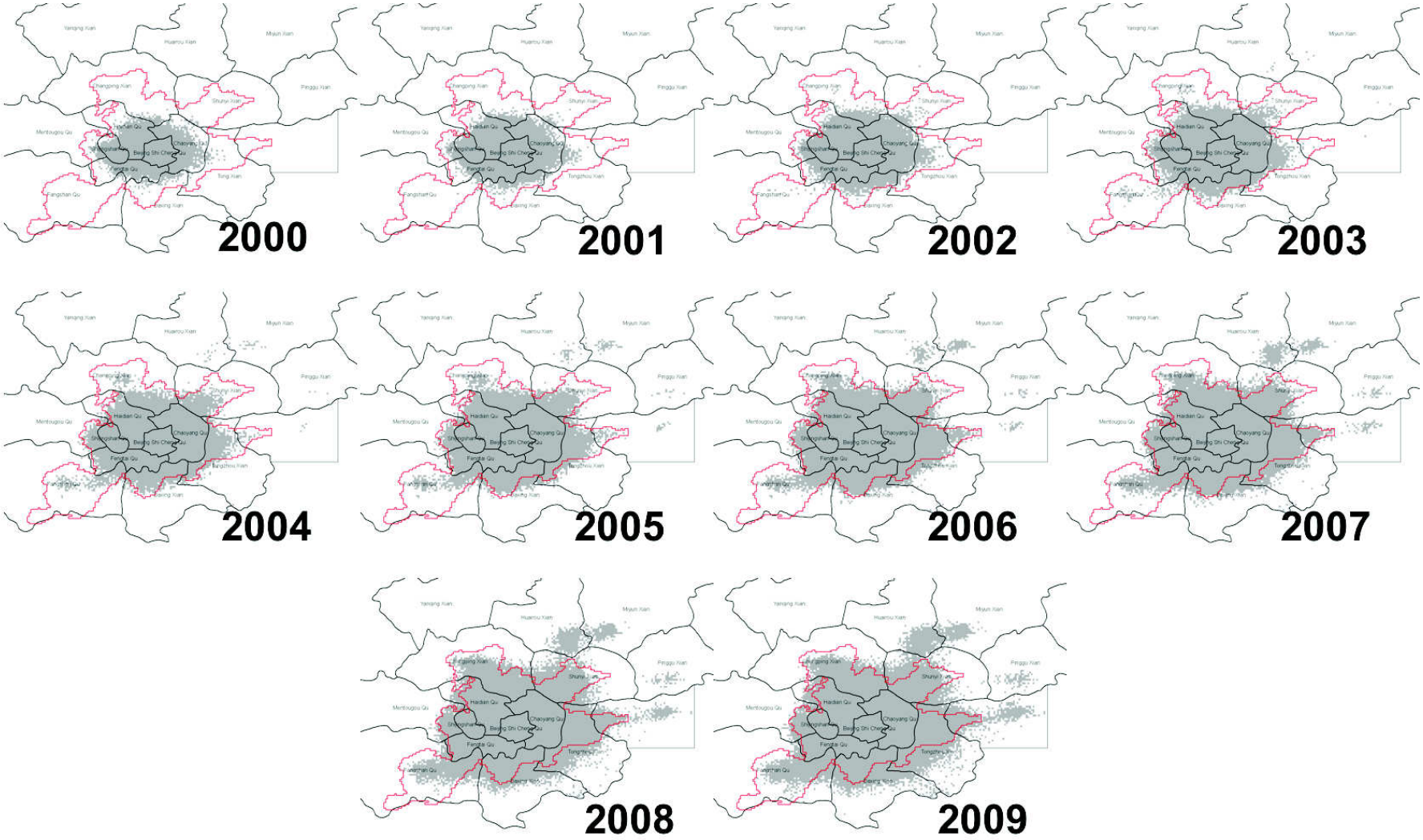

Paper in preparation

Beijing Urban Change and NO_2

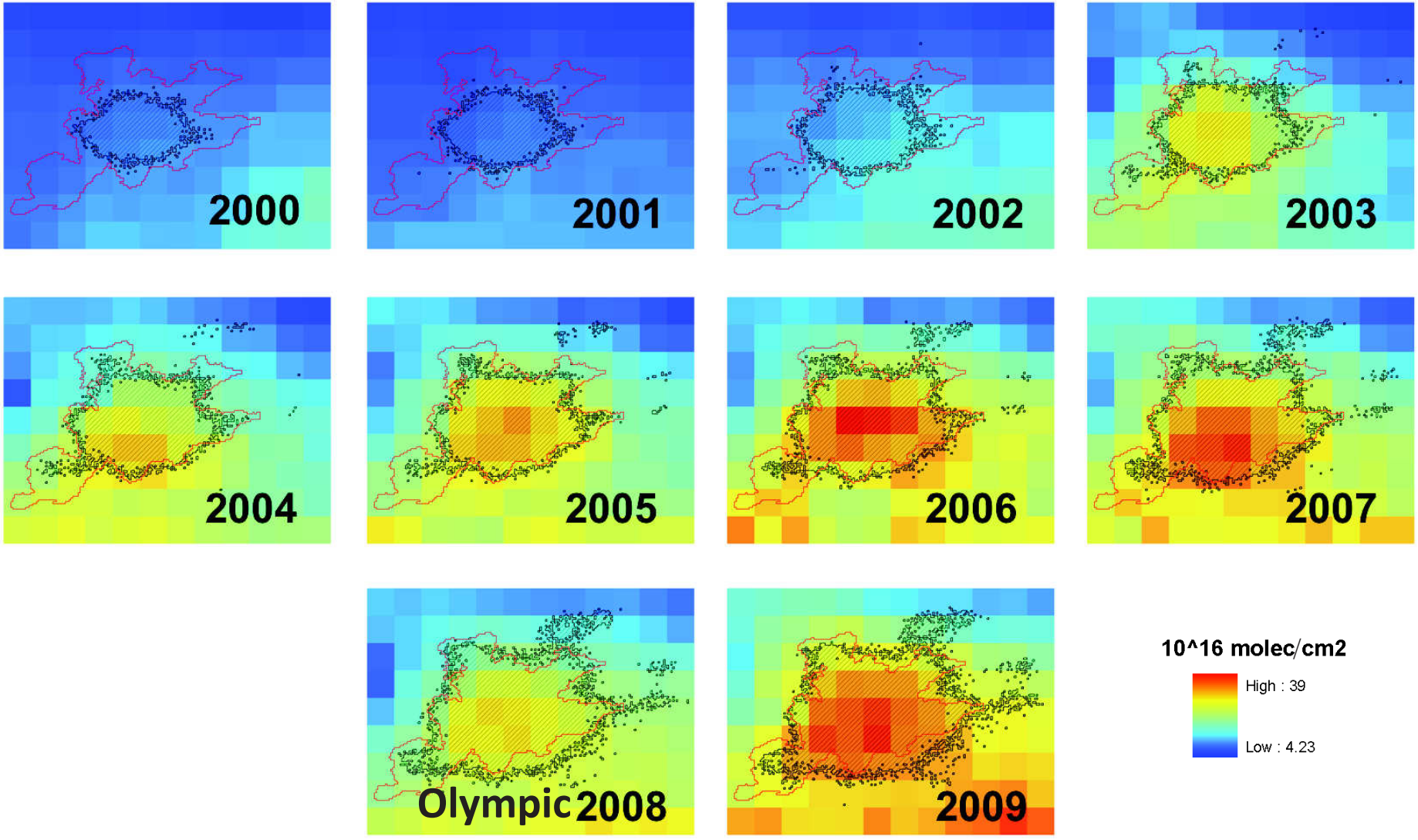

Paper in preparation

Increase Information Content with Multiple Satellite Data

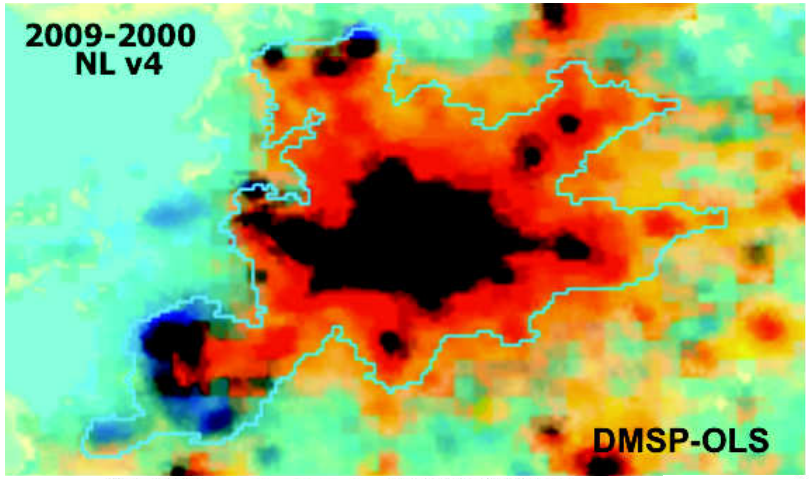

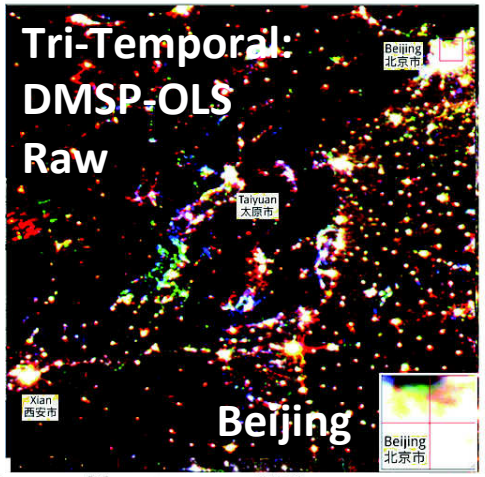

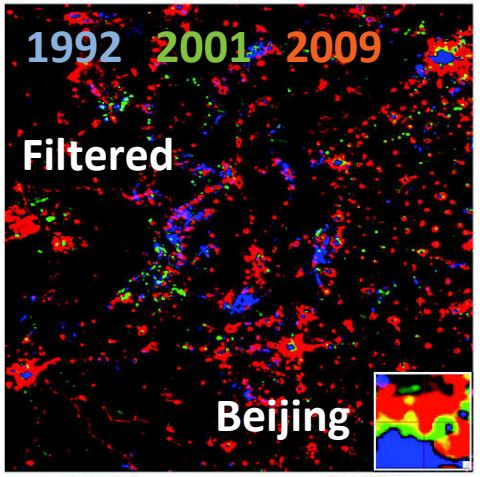

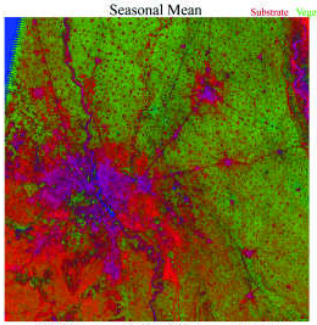

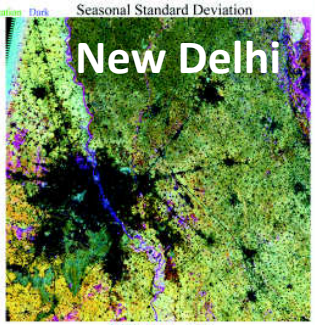

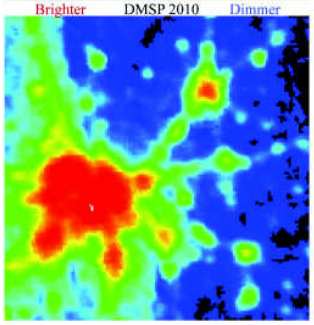

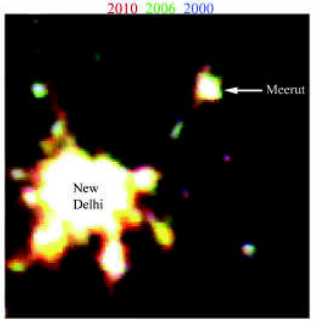

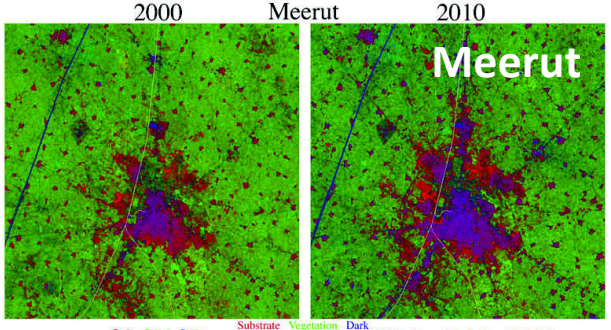

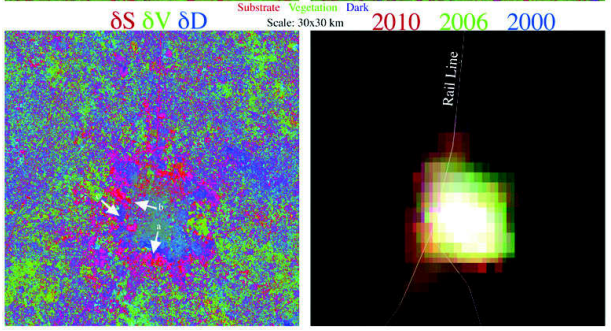

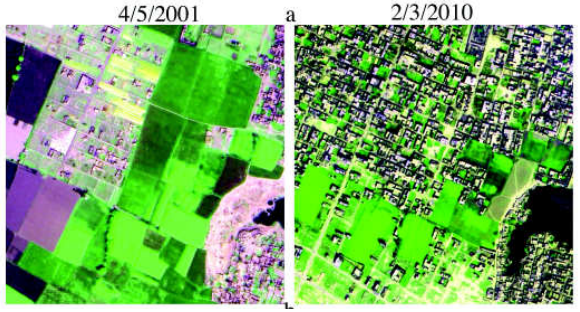

See poster by Small et al., LCLUC, 2014

Demography – Population Change in 2000-2010

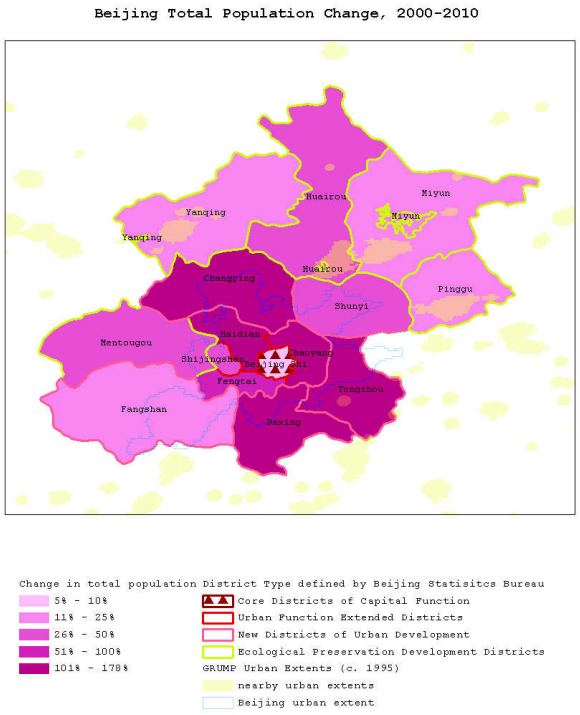

Beijing total population change

- **Highest rate of total population growth in districts called "New Districts of Urban Development" surrounding the city proper.**
- **Growth rate of migrant population is much higher than the growth rate of native population.**
- **Growth of native urban population is slow, and probably is an indicator of strict "Hukou" registration system.**

Results from Balk

Infrastructure – Road Network

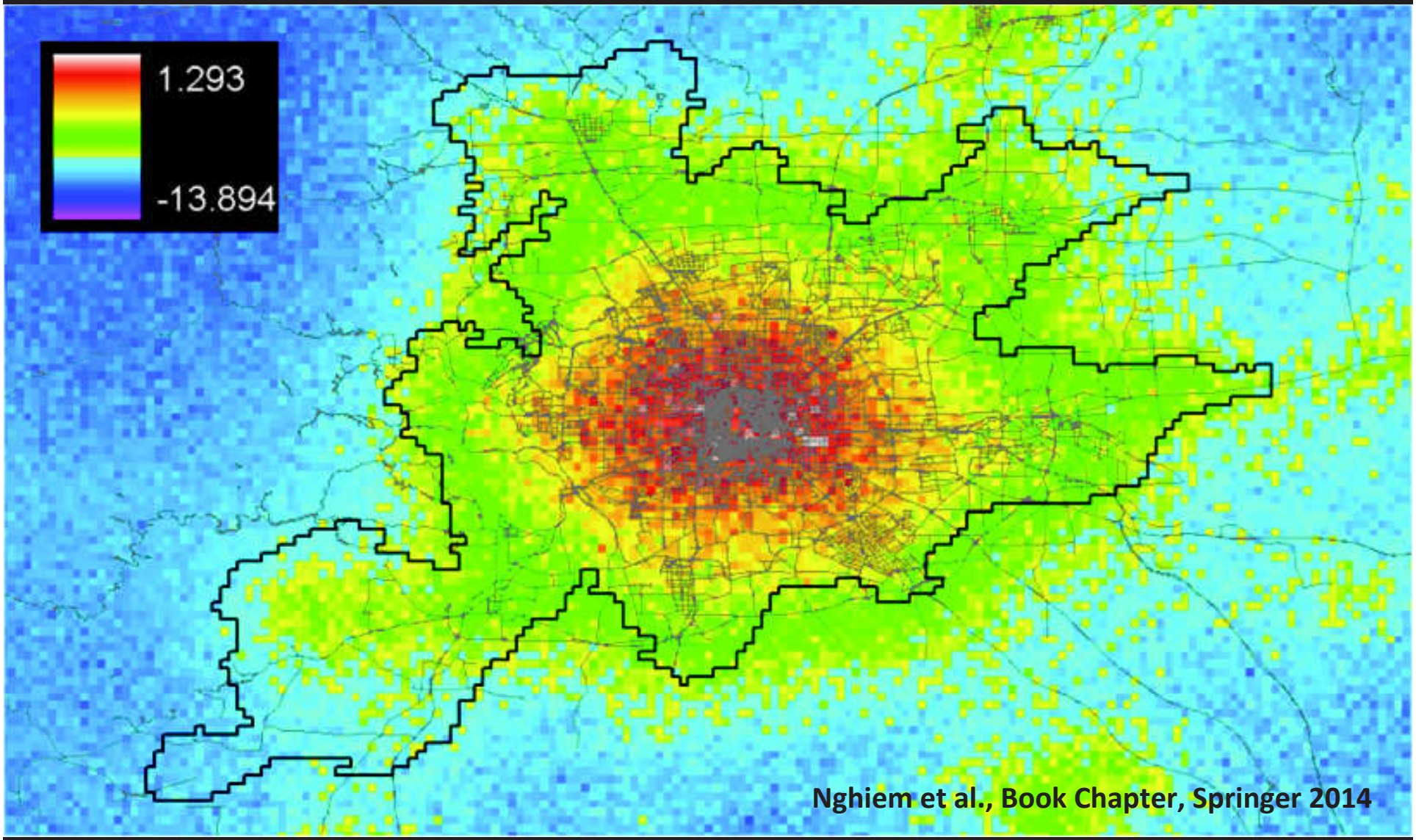

Beijing DSM with road network (grey) and Night-Light urban extent (black).

Modeling – GATOR-GCMOM
from global circulation to urban scale

- **GATOR-GCMOM is used to simulate the global, regional, and urban climate and air pollution health impacts resulting from urbanization. The goal is to investigate effects on climate and air quality of annual changes in the extent of urbanization over regions of mega urbanization in Asia and to compare with other regions in the 2000s.**

- **This model nests climate, meteorological, gas, aerosol, and radiative parameters simultaneously from the global through urban scale. simulates meteorology and its feedback among gases, aerosol particles, cloud hydrometeor particles, surfaces, and radiation. Gas processes include emissions, photochemistry, gas-to-particle conversion, gas-to-hydrometeor conversion and exchange, gas-ocean exchange, advection, convection, molecular diffusion, turbulent diffusion, and dry deposition.**

- **At the land surface, each subgrid soil class is divided into vegetated and bare soil. Snow can accumulate on both soil and vegetation. For bare and vegetated soil, the surface energy balance equation accounts for latent heat, sensible heat, solar, thermal-IR, and energy fluxes.**

- **Oceans are represented in 3-D for some calculations and 2-D for others. A 2-D time-dependent mixed-layer ocean dynamics model driven by surface wind stress is used to solve for mixed-layer velocities, heights, and horizontal energy transport in each cell. The scheme conserves potential enstrophy, vorticity, energy, and mass and predicts gyres and major currents. Air ocean exchange, vertical diffusion, 3-D ocean equilibrium chemistry and pH are solved among the Na-Cl-Mg-Ca-K-H-O-Li-Sr-C-S-N-Br-F-B-Si-P system.**

Modeling from Jacobson

Modeling – GATOR-GCMOM
Mega urbanization impacts in 2000s

Quantifying changes in 2000-2009

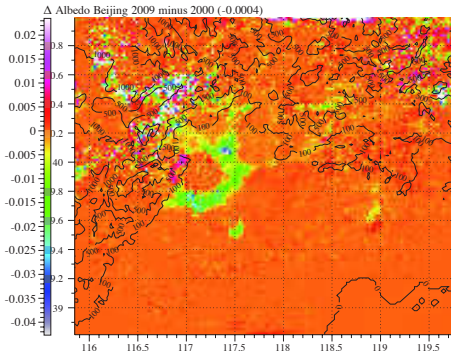

Albedo Change

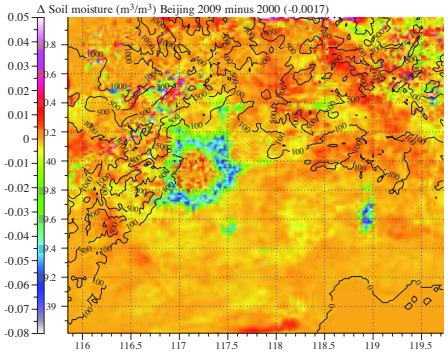

Soil Moisture Change

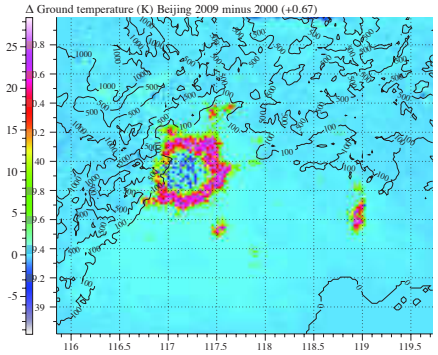

Ground Temperature

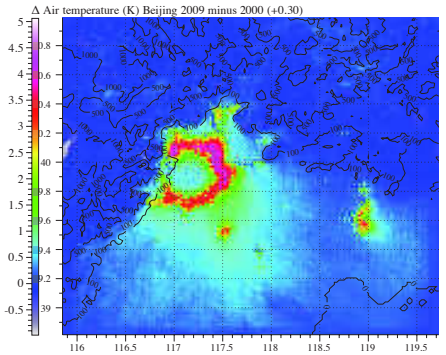

Surface Air Temperature

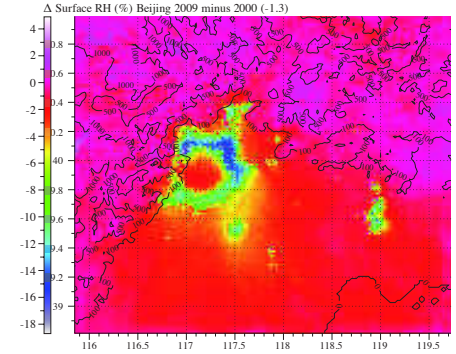

Surface Rel. Humidity

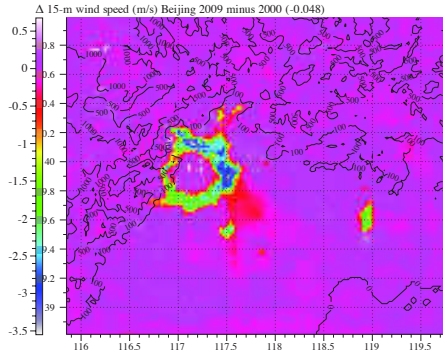

15-m Wind Speed

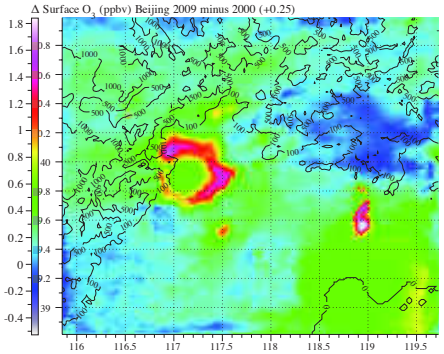

Surface Ozone

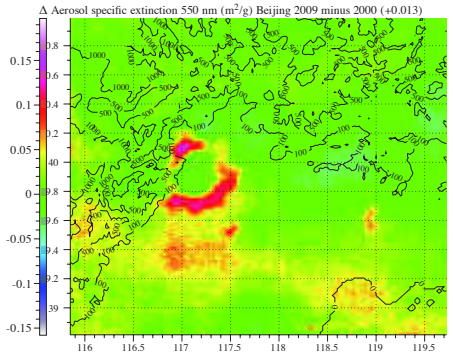

Aerosol Spc. Extinction

Model results from Jacobson

Model – GATOR-GCMOM
Mega urbanization impacts in 2000s

"Ring Around the Beijing"

- Increasing urban heat
- Drier soil condition
- More air stagnation
- Worse smog condition
- More ozone pollution
- More pollutant mixing upward

Model results from Jacobson

Formation of Mega-Agglomeration
Challenging the Westphalian System

Changes between 2000 and 2009

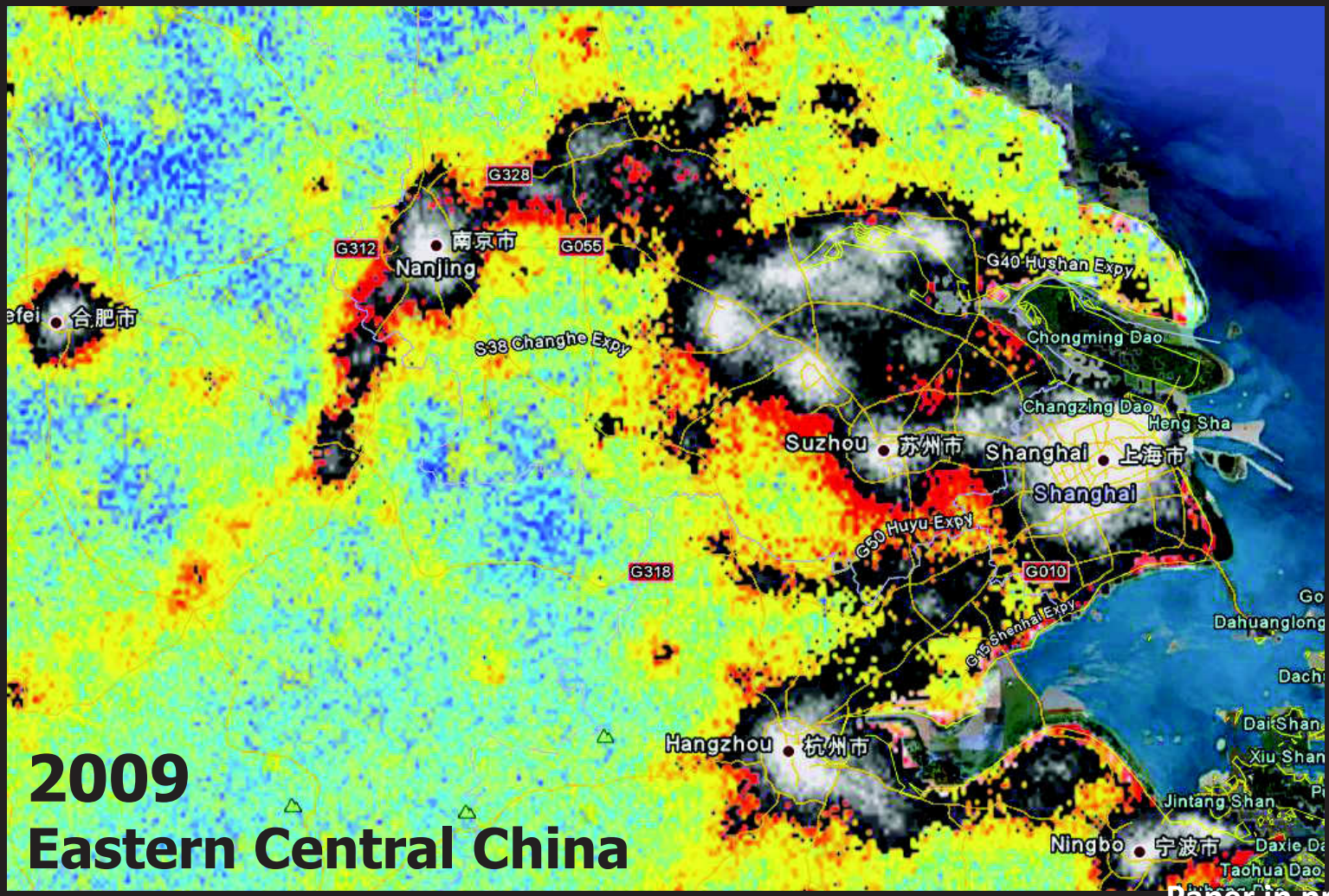

Paper in preparation

DSM Assessment of Ground-Water Contamination

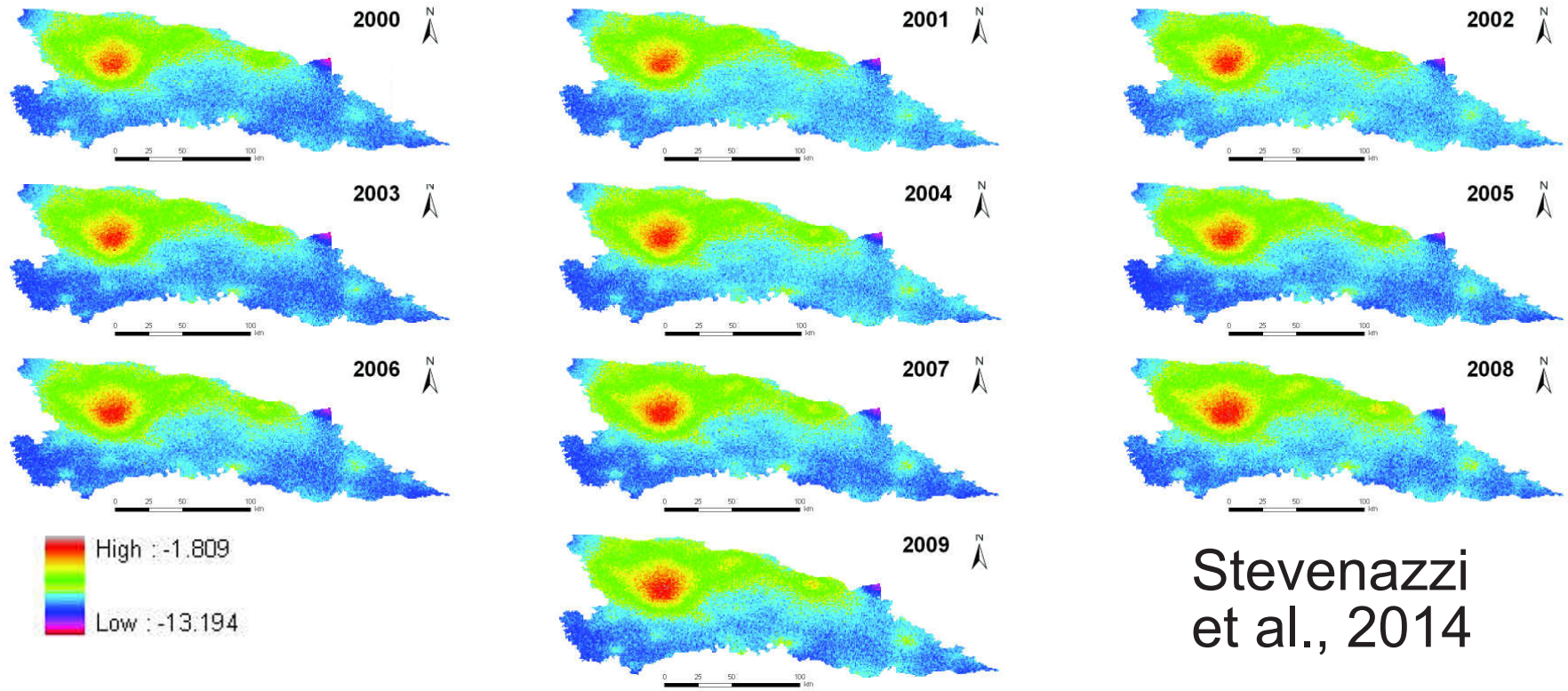

Stevenazzi et al., 2014

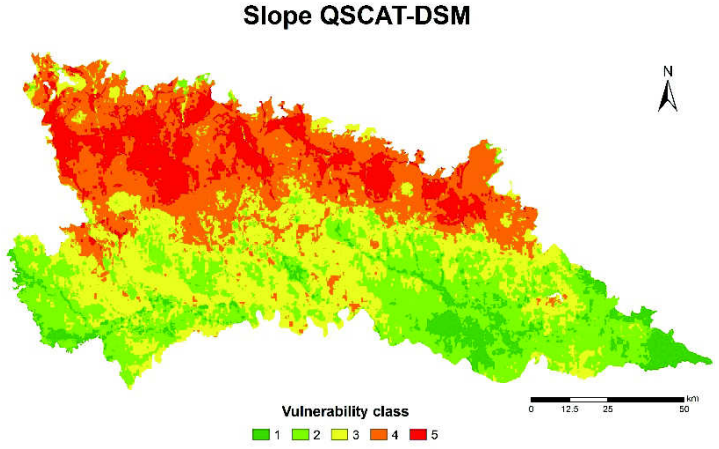

Nitrate Monitoring Wells

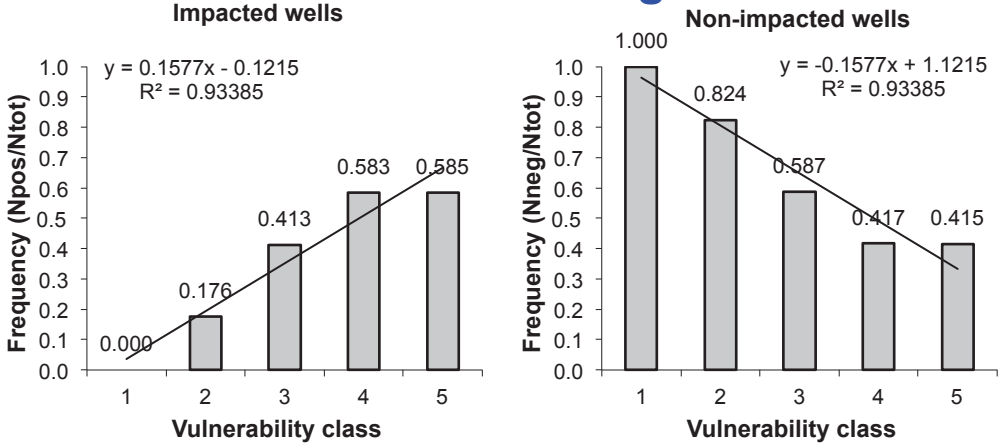

POPLEX Field Campaign
2-17 May 2014, Italy
22 participants, 14 institutions, 5 countries, 12 satellites, many in-situ networks

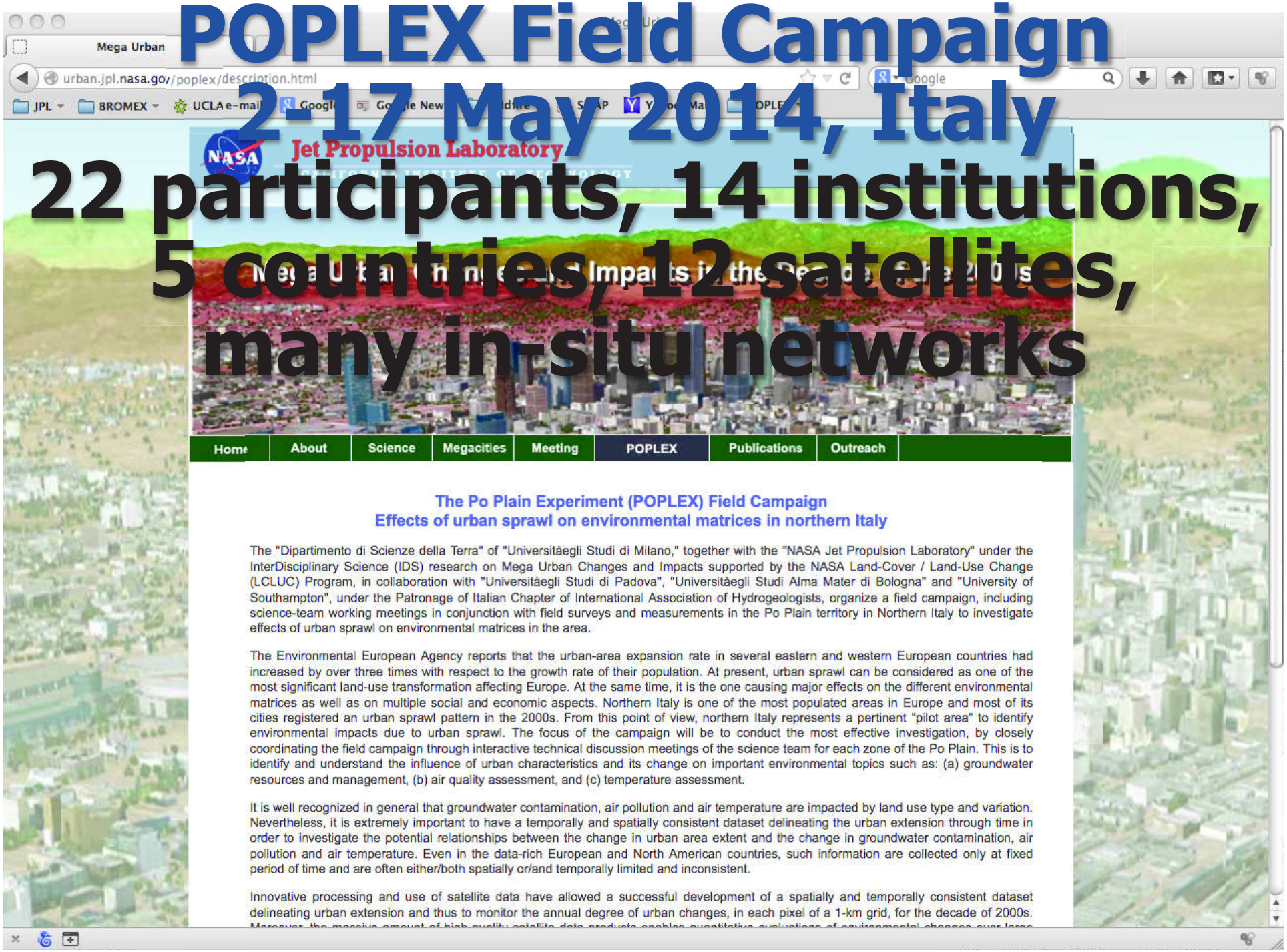

Contact

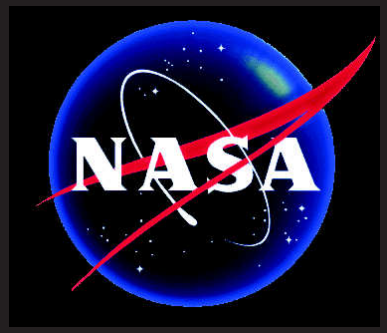

Son.V.Nghiem@jpl.nasa.gov